



Published in final edited form as:

*Bioorg Med Chem Lett.* 2008 August 1; 18(15): 4312–4315. doi:10.1016/j.bmcl.2008.06.087.

## Molecular Modeling of a PAMAM-CGS21680 Dendrimer Bound to an A<sub>2A</sub> Adenosine Receptor Homodimer

Andrei A. Ivanov and Kenneth A. Jacobson

*Molecular Recognition Section, Laboratory of Bioorganic Chemistry, National Institute of Diabetes and Digestive and Kidney Diseases, National Institutes of Health, Bethesda, Maryland 20892, USA.*

### Abstract

The theoretical possibility of bivalent binding of a dendrimer, covalently appended with multiple copies of a small ligand, to a homodimer of a G protein-coupled receptor was investigated with a molecular modeling approach. A molecular model was constructed of a third generation (G3) poly (amidoamine) (PAMAM) dendrimer condensed with multiple copies of the potent A<sub>2A</sub> adenosine receptor agonist CGS21680. The dendrimer was bound to an A<sub>2A</sub> adenosine receptor homodimer. Two units of the nucleoside CGS21680 could occupy the A<sub>2A</sub> receptor homodimer simultaneously. The binding mode of CGS21680 moieties linked to the PAMAM dendrimer and docked to the A<sub>2A</sub> receptor was found to be similar with the binding mode of a monomeric CGS21680 ligand.

G protein-coupled receptors (GPCRs) are transmembrane proteins which comprise a large and diverse superfamily of proteins. These receptors consist of seven transmembrane  $\alpha$ -helices (TMs) connected by three extracellular and three intracellular loops. Besides the evidence that some GPCRs can function as monomeric units<sup>1</sup>, mounting evidence supports the critical functional role of homo- and heterodimerization and oligomerization of GPCRs.<sup>2</sup> It was shown that homo- and heterodimerized GPCRs display different pharmacological properties as compared with monomeric receptors.<sup>3</sup>

It was proposed that GPCR dimers can be activated or inhibited by bivalent ligands.<sup>4</sup> In general, a bivalent ligand consists of two pharmacophore units connected by a spacer.<sup>5</sup> Theoretically, but not necessarily, such bivalent ligands could occupy each of two units of a GPCR dimer simultaneously. Numerous studies have addressed to the design of bivalent ligands for GPCRs, and several examples of potent bivalent ligands were reported for various receptors, including opioid, serotonin, muscarinic and other receptors.<sup>6,7</sup>

Recently, we have demonstrated that GPCRs can be activated not only by monomeric or bivalent ligands, but also by multivalent ligands. We have reported that intracellular signal transduction across the A<sub>2A</sub> adenosine receptor (AR) can be induced by the A<sub>2A</sub> AR agonist 2-[4-(2-carboxylethyl)phenylethylamino]-5'-N-ethylcarboxamidoadenosine (CGS21680 **1**) coupled covalently to a PAMAM dendrimer.<sup>8</sup> A<sub>2A</sub> AR agonists are known to display a potent antiaggregatory effect in human platelet preparations. Our functional assay clearly demonstrated a potent antiaggregatory effect of the PAMAM-CGS21680 dendrimer on platelet aggregation.

Correspondence to: Kenneth A. Jacobson.

**Publisher's Disclaimer:** This is a PDF file of an unedited manuscript that has been accepted for publication. As a service to our customers we are providing this early version of the manuscript. The manuscript will undergo copyediting, typesetting, and review of the resulting proof before it is published in its final citable form. Please note that during the production process errors may be discovered which could affect the content, and all legal disclaimers that apply to the journal pertain.

However, there is no experimental evidence that CGS21680 units coupled to the PAMAM dendrimer can occupy more than one subunit of the A<sub>2A</sub> AR simultaneously. In the present study we utilize computational molecular modeling to investigate if the bivalent binding of PAMAM-CGS21680 to an A<sub>2A</sub> AR dimer is theoretically allowed.

At the first stage, the molecular docking of CGS21680 **1** to the A<sub>2A</sub> AR monomer was performed automatically with the Glide XP software.<sup>9</sup> Our recently published molecular model of (*E*)-*N*-ethyl-1'-deoxy-1'-[6-amino-2-(5-phenyl-1-penten-1-yl)-9H-purin-9-yl]-β-D-ribofuranuronamide (2-phenylpentenyl-NECA) bound to the A<sub>2A</sub> AR was utilized for the docking studies.<sup>10</sup> The Protein Preparation Wizard of the MacroModel software<sup>11</sup> with its default parameters was used to prepare the model of the A<sub>2A</sub> AR for the Glide calculations. The center of the box for the molecular docking of CGS21680 was placed in the center of 2-phenylpentenyl-NECA. The length of 28.44 Å was used for all box sides. Since the binding site of the initial A<sub>2A</sub> AR model was optimized to fit 2-phenylpentenyl-NECA, which is a structurally similar to CGS21680, no additional refinement of the receptor binding site was performed. Not surprisingly, the binding mode of CGS21680 at the A<sub>2A</sub> AR was found to be similar to the binding mode of 2-phenylpentenyl-NECA and to other agonists of ARs.<sup>11–15</sup> In particular, His278 (7.43) appeared in proximity to the 2'- and 3'-hydroxyl groups of the ligand (see Supplementary data). Amino acid residue numbers shown in parentheses correspond to the Ballesteros-Weinstein numbering system that relates its relative position on a particular helix.<sup>16</sup> Thr88 (3.36) and Ser277 (7.42) were involved in H-bonding interactions with the amido group of the *N*-ethylcarboxamido moiety. The N<sup>6</sup>-amino group of CGS21680 formed an H-bond with Asn253 (6.55). In addition, the carboxylic oxygen atom of the 2-[4-(2-carboxylethyl)phenylethylamino] moiety of the ligand established an H-bond with Asn145 (EL2), and the phenyl ring of that moiety could be involved in the π-π interactions with the aromatic ring of Phe168 (EL2).

After molecular docking of CGS21680 to the A<sub>2A</sub> AR, the *N*-(2-aminoethyl)-3-(dimethylamino)propanamide chain was attached to the carboxylic group of the ligand to build the ligand **2** (Figure 1). To take into account the hydrophobic nature of the methylene groups of PAMAM, a 3-(dimethylamino)propanamide fragment was used instead of a 3-(amino)propanamide moiety. The Monte Carlo Multiple Minimum conformational search analysis (MCM) was utilized to obtain the most favorable conformation and orientation of the ligand inside the A<sub>2A</sub> AR. The ligand and all residues located within 5 Å around the ligand were subjected to MCM calculations with a shell of constrained residues located within an additional 2 Å. The following parameters were used: MMFFs force field, water as an implicit solvent, maximum of 500 iterations of the Polak-Ribier conjugate gradient (PRCG) minimization method with a convergence threshold of 0.05 kJ·mol<sup>-1</sup>·Å<sup>-1</sup>, number of conformational search steps = 100, energy window for saving structures = 100 kJ·mol<sup>-1</sup>. The results of MCM calculations indicated that the long chain at the position 2 of the adenine ring of the ligand is oriented toward the extracellular part of the receptor. In particular, in the model obtained the *N*-(2-aminoethyl)-3-(dimethylamino)propanamide moiety was located between the extracellular parts of TM4 and TM5 of the A<sub>2A</sub> AR. Moreover, the terminal amino group of this chain was found outside the receptor.

The model of the A<sup>2A</sup> AR with the docked ligand **2** was used to build a model of the A<sub>2A</sub> AR homodimer, for which physical evidence was reported.<sup>2b</sup> With this aim our recently published model of the A<sub>3</sub> AR homodimer was utilized as a template.<sup>17</sup>

The A<sub>2A</sub> AR monomer with the ligand docked inside was duplicated and superimposed with each subunit of the A<sub>3</sub> AR dimer using the Protein Structure Alignment tool implemented in the MacroModel software. Then, the geometry of the A<sub>2A</sub> AR side chains was optimized by

energy minimization in the MMFFs force field. The PRCG minimization method was used. The resulting model of the A<sub>2A</sub> AR dimer is shown in Figure 2.

The initial model of the A<sub>2A</sub> AR was built based on the X-ray structure of rhodopsin, and as in rhodopsin, EL2 of the A<sub>2A</sub> AR covers the binding site to prevent exit of a ligand from the receptor. However, as shown in Figure 2, the *N*-(2-aminoethyl)-3-(dimethylamino) propanamide chain of **2** was located under EL2 and oriented toward the upper parts of TM4 and TM5 in the model. Such an orientation of the ligand **2** allows its *N*-(2-aminoethyl)-3-(dimethylamino)propanamide moiety to be outside the receptor without significant changes in the structure of EL2.

As shown in Figure 2, the terminal amino groups of the ligands **2** located inside the receptor subunits were oriented toward each other. However, the distance between the nitrogen atoms of the amino groups was found to be 11.2 Å. Thus it is unlikely that the A<sub>2A</sub> AR dimer subunits can be occupied by CGS21680 units, if they are closest neighbors on one branch of the PAMAM dendrimer. For this reason, the second 3-(dimethylamino)-*N*-ethylpropanamide chain was attached to the terminal nitrogen atoms of the ligands **2** docked to each dimer subunit providing ligand **3**. The length and flexibility of the poly(amidoamine) chains connected to CGS21680 allowed us to manually adjust the conformation of these chains to superimpose their terminal nitrogen atoms. Then, the terminal nitrogen atom of one ligand was deleted and a remaining terminal ethylene group of this ligand was connected to the terminal nitrogen atom of the second ligand. This resulted in compound **4** bound to the A<sub>2A</sub> AR dimer. To refine the geometry of the model, the obtained bivalent ligand bound to the A<sub>2A</sub> AR dimer was subjected to MCMM calculations with the same parameters as described above. Then, two additional CGS21680 moieties with amidoamine chains attached, and an additional 3-(dimethylamino)-*N*-ethylpropanamide fragment were connected to ligand **4** resulting in compound **5** (Figure 1). The geometry of the model was optimized by energy minimization (Figure 3).

In parallel to the molecular modeling of the A<sub>2A</sub> AR dimer, a model of the PAMAM G3 dendrimer was constructed. With this aim, the 3-dimensional structure of the PAMAM generation 0 (G0) was sketched with the MacroModel software and subjected to MCMM calculations. The number of the conformational search steps was set to 500, and the energy window for saving structures of 500 kJ·mol<sup>-1</sup> was used. The resulting model of the G0 dendrimer was used as a starting structure to build a model of the entire PAMAM G3 dendrimer. The PAMAM generations G1, G2, and G3 were obtained by manual attachment of corresponding amidoamine chains to the previous generation followed by optimization of the geometry with MCMM calculations.

The compactness of a polymer structure can be characterized by the value of its radius of gyration. The radius of gyration is calculated as:

$$R_g = \left( \frac{\sum_i \|r_i\|^2 m_i}{\sum_i m_i} \right)^{\frac{1}{2}}$$

where  $m_i$  is the mass of atom  $i$  and  $r_i$  is the position of atom  $i$  with respect to the center of mass of the molecule. The value of  $R_g$  of the PAMAM G3 molecular model obtained after MCMM calculations was calculated with the GROMACS software<sup>18</sup> and was found to be 1.64 nm. The calculated value of  $R_g$  is in good agreement with the experimental value of  $R_g = 1.58$  nm measured with the small-angle X-ray scattering (SAXS) method.<sup>19</sup> In order to quantitatively characterize the overall shape of the PAMAM G3 dendrimer the ratio of the principal moments of inertia ( $I_z/I_x$  and  $I_z/I_y$ ) were calculated.  $I_x$ ,  $I_y$ , and  $I_z$  represent the eigenvalues of the radius of gyration tensor  $S$ , and  $I_x \leq I_y \leq I_z$ .<sup>20</sup> The obtained values of  $I_z/I_y = 1.5$  and  $I_z/I_x = 1.1$  suggested that the model of PAMAM dendrimer has a compact spherical structure. In addition, the value

of relative shape anisotropy was calculated as  $k^2 = 1 - 3I_2/I_1^2$ , where  $I_1 = I_x + I_y + I_z$  is the first invariant of  $S$ , and  $I_2 = I_x I_y + I_y I_z + I_x I_z$  is the second invariant of  $S$ . For a linear array of skeletal atoms  $k^2 = 1$ , and for structures of high 3-dimensional symmetry  $k^2 = 0$ . The value of  $k^2$  calculated for the PAMAM G3 molecular model was found to be  $k^2 = 0.012$  also indicating compact spherical structure of the dendrimer.

Since the model of PAMAM dendrimer obtained after MCMM calculations demonstrated a reasonable size and shape it was used for the conjugation with CGS21680 units. Multiple copies of CGS21680 moieties were connected to the terminal amino groups of the PAMAM model to build a model of full substituted PAMAM-CGS21680. To avoid the overlapping of the CGS21680 units with the amidoamine chains of the dendrimer the initial orientation of CGS21680 moieties was manually adjusted. Then, the model was optimized by a MCMM conformational search analysis (Figure 4).

In order to combine the models of the  $A_{2A}$  AR dimer and PAMAM-CGS21680 dendrimer, the following procedure was performed. A dendron fragment of dendrimer **6**, corresponding to ligand **5** excluding the terminal dimethylamino group was removed from **6**. In turn, the terminal dimethylamino group was removed from ligand **5** in its docked conformation at the  $A_{2A}$  AR homodimer. Then, the abovementioned truncated dendrimer conjugate was connected to the remaining terminal ethylene group of ligand **5**, to complete the structure of **6** docked in the receptor. In the model obtained, several chains of PAMAM-CGS21680 overlapped with the  $A_{2A}$  AR structure. The conformation of those chains was manually adjusted, and the model was subjected to the energy minimization. Then, a randomly selected CGS21680 unit was replaced by the fluorophore (Alexa Fluor 488) molecule providing dendrimer **6**. The model geometry was refined by energy minimization followed by 100 ps of molecular dynamics (MD) simulation. The MD simulation was performed with the MacroModel software. The following parameters of the MD simulation were used: force field MMFFs, water as an implicit solvent, a maximum of 500 iterations of the Polak-Ribier conjugate gradient (PRCG) minimization method with a convergence threshold of  $0.05 \text{ kJ}\cdot\text{mol}^{-1}\cdot\text{\AA}^{-1}$ , SHAKE constraints for all bonds to hydrogen atoms, simulation temperature of 300.0 K, time step of 1.0 fs, equilibration time of 1.0 ps, simulation time of 100.0 ps. The final molecular model of the PAMAM-CGS21680 bound to the  $A_{2A}$  AR dimer is shown in Figure 5.

After the MD simulation, the analysis of the binding mode of CGS21680 units located inside the  $A_{2A}$  AR dimer was performed. The binding mode of each subunit was found to be similar as compared with the initial model of CGS21680 docked to the  $A_{2A}$  AR and remained in agreement with the data of site-directed mutagenesis.<sup>21</sup> These results confirmed the principal possibility for the  $A_{2A}$  AR homodimer subunits to be occupied at the same time by two CGS21680 units conjugated with the PAMAM G3 dimer.

To summarize, the first molecular model of the  $A_{2A}$  AR homodimer has been proposed and utilized for the molecular docking of a potent agonist of the  $A_{2A}$  AR – CGS21680. The molecular models of pure PAMAM G3 dendrimer and PAMAM-CGS21680 have been constructed. The overall shape and size of the PAMAM G3 model was found in good agreement with available experimental data. The molecular model of PAMAM – CGS21680 bound to the  $A_{2A}$  AR dimer was proposed for the first time. It was shown that both subunits of the  $A_{2A}$  AR dimer can be occupied simultaneously by CGS21680 moieties of the PAMAM-CGS21680 dendrimer. We believe that these results can be useful for further investigation of interactions between GPCRs and dendrimer macromolecules and for the rational design of novel multivalent ligands for ARs and other GPCR homo- and heterodimers.

## Supplementary Material

Refer to Web version on PubMed Central for supplementary material.

## Acknowledgements

This research was supported by the Intramural Research Program of the NIH, National Institute of Diabetes & Digestive & Kidney Diseases. We thank Athena M. Klutz and Dr. Yoonkyung Kim for helpful discussions.

## References

1. Chabre M, le Maire M. *Biochemistry* 2005;44:9395. [PubMed: 15996094]
2. a) Franco R, Casadó V, Cortés A, Mallol J, Ciruela F, Ferré S, Lluís C, Canela E. *Br. J. Pharmacol* 2008;153:S90. [PubMed: 18037920] b) Canals M, Burgueno J, Marcellino D, Cabello N, Canela E, Mallol J, Agnati L, Ferré S, Bouvier M, Fuxe K, Ciruela F, Lluís C, Franco R. *J. Neurochem* 2004;88:726. [PubMed: 14720222]
3. Maggio R, Novi F, Scarselli M, Corsini GU. *FEBS J* 2005;272:2939. [PubMed: 15955054]
4. Jacobson KA, Xie R, Young L, Chang L, Liang BT. *J. Biol. Chem* 2000;275:30272. [PubMed: 10887176]
5. Morphy R, Rankovic Z. *J. Med. Chem* 2005;48:6523. [PubMed: 16220969]
6. Messer WS Jr. *Curr. Pharm. Des* 2004;10:2015. [PubMed: 15279542]
7. Zhang A, Liu Z, Kan Y. *Curr. Top. Med. Chem* 2007;7:343. [PubMed: 17305575]
8. Kim Y, Hechler B, Klutz AM, Gachet C, Jacobson KA. *Bioconjug. Chem* 2008;19:406. [PubMed: 18176997]
9. Glide, version 4.5. New York, NY: Schrödinger, LLC; 2007.
10. Kim S-K, Gao Z-G, Van Rompaey P, Gross AS, Chen A, Van Calenbergh S, Jacobson KA. *J. Med. Chem* 2003;46:4847. [PubMed: 14584936]
11. MacroModel, version 9.5. New York, NY: Schrödinger, LLC; 2007.
12. Costanzi S, Ivanov AA, Tikhonova IG, Jacobson KA. *Front. Drug. Des. Discov* 2007;3:63.
13. Palaniappan KK, Gao ZG, Ivanov AA, Greaves R, Adachi H, Besada P, Kim HO, Kim AY, Choe AA, Jeong LS, Jacobson KA. *Biochemistry* 2007;46:7437. [PubMed: 17542617]
14. Ivanov AA, Wang B, Klutz AM, Chen VL, Gao ZG, Jacobson KA. *J. Med. Chem* 2008;51:2088. [PubMed: 18321038]
15. Ivanov AA, Palyulin VA, Zefirov NS. *J. Mol. Graph. Mod* 2007;25:740.
16. Ballesteros JA, Weinstein H. *Methods Neurosci* 1995;25:366.
17. Kim S-K, Jacobson KA. *J. Mol. Graph. Mod* 2006;25:549.
18. van der Spoel D, Lindahl E, Hess B, Groenhof G, Mark AE, Berendsen HJC. *J. Comp. Chem* 2005;26:1701. [PubMed: 16211538]
19. Prosa TJ, Bauer BJ, Amis EJ, Tomalia DA, Scherrenberg R. *J. Polymer. Sci. B* 1997;35:2913.
20. Theodorou DN, Suter UW. *Macromolecules* 1985;18:1206.
21. Duong HT, Gao ZG, Jacobson KA. *Nucleos. Nucleot. Nucleic Acids* 2005;24:1507.

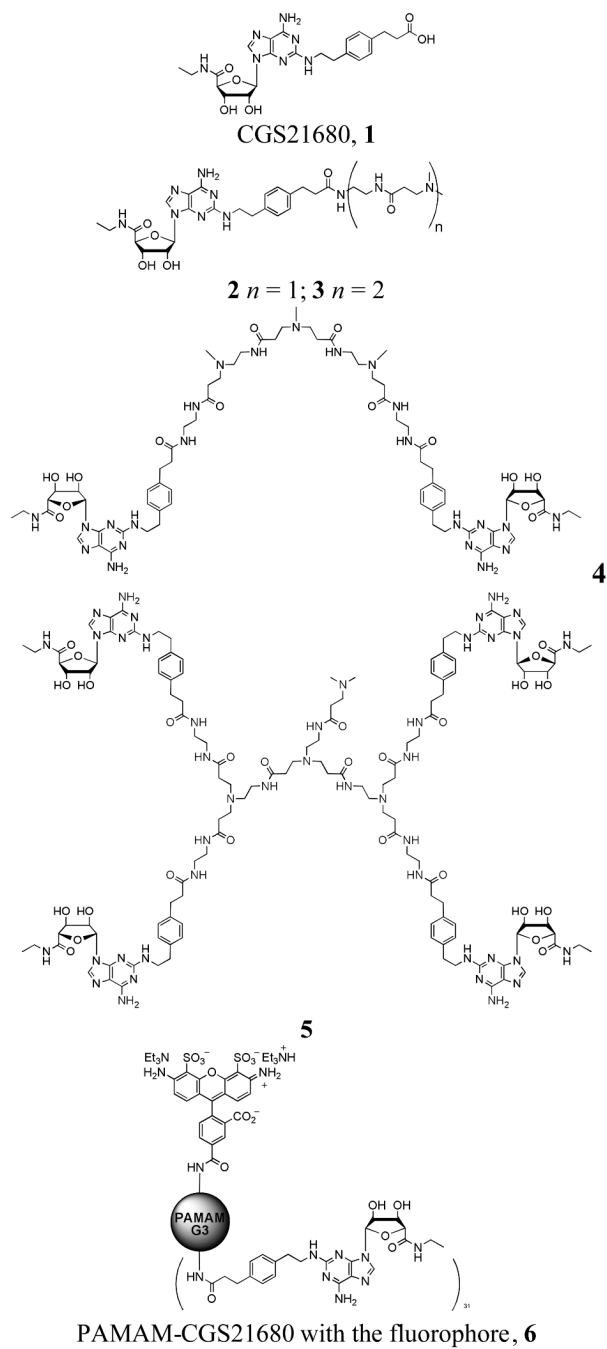


**Figure 1.** The molecules and conjugates used in molecular docking studies. The entire chemical structure of **6** is provided in Supplementary data.

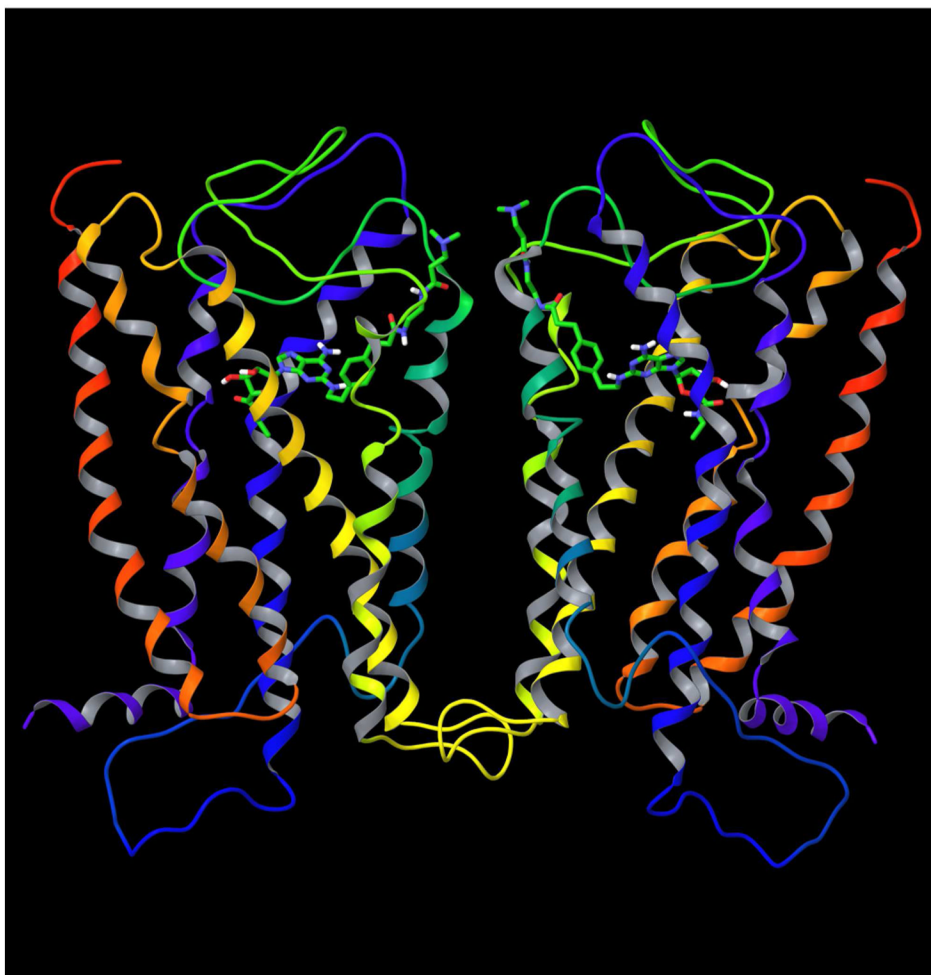


**Figure 2.**  
The molecular model of the A<sub>2A</sub> AR homodimer with the compound **2** inside.



**Figure 3.**  
The ligand **5** docked to the A<sub>2A</sub> AR homodimer.



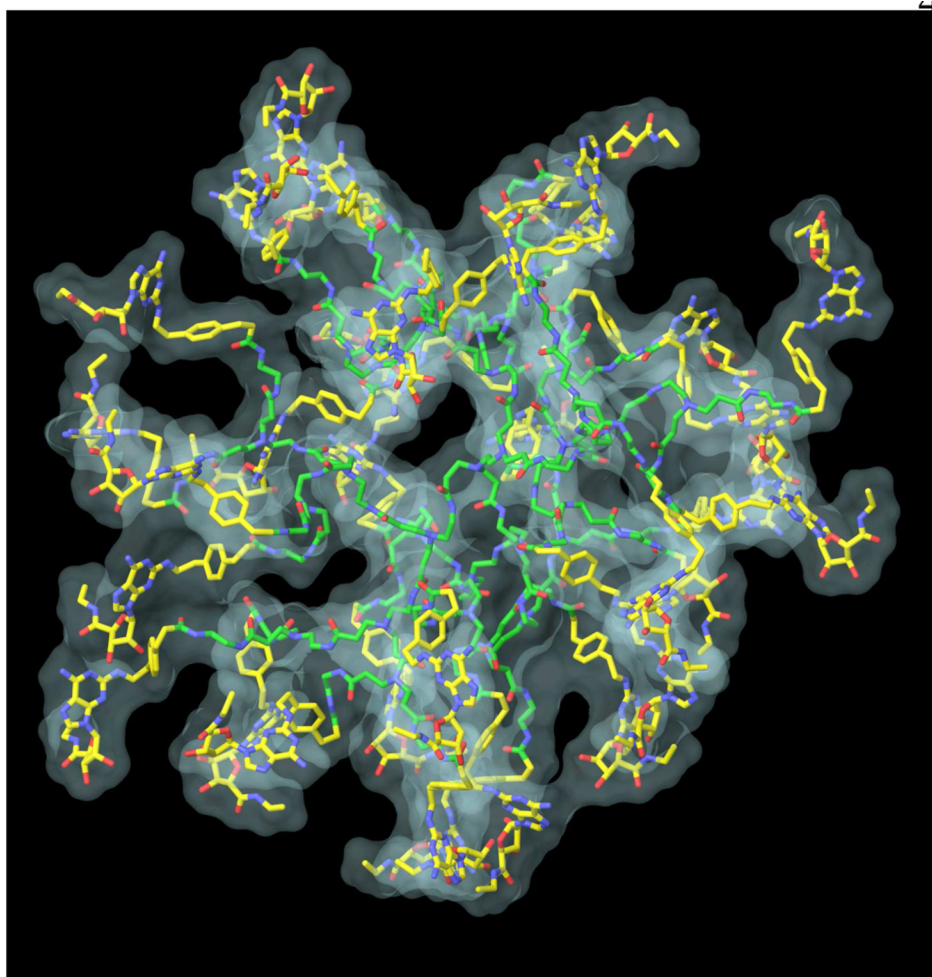


**Figure 4.** Molecular model of PAMAM-CGS21680 dendrimer obtained after MCM calculations. The carbon atoms of PAMAM are colored in green, and carbon atoms of CGS21680 units are colored in yellow. Also, the molecular surface of the dendrimer is shown.

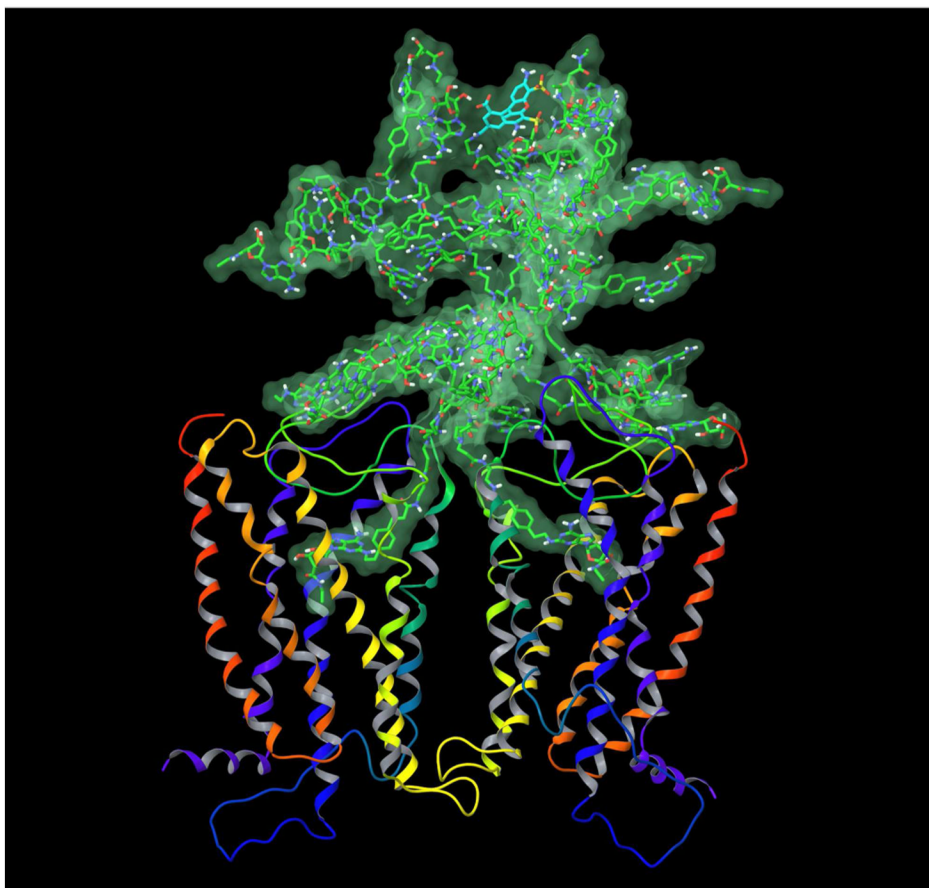


**Figure 5.** The final model of PAMAM-CGS21680 with the fluorophore, **6** bound to the A<sub>2A</sub> AR homodimer. The carbon atoms of PAMAM and CGS21680 units are colored in green, carbon atoms of fluorophore are colored in cyan. The distances between the ribose ring oxygens (34.96 Å) and between C $\alpha$  atoms of the N-terminal Met residue of each A<sub>2A</sub> subunit (66.86 Å) were measured. The overall height of the complex of the receptor dimer with the dendrimer bound is about 110 Å.